

# The Principle of Effect of the Transient Gain Reduction and Its Effect on Tuning Power System Stabilizer

Ghazanfar Shahgholian<sup>1</sup>, Mehdi Mehdavian<sup>2</sup>, Manijeh Azadeh<sup>2</sup>, Saeed Farazpey<sup>2</sup>, Mohammadreza Janghorbani<sup>3</sup>

<sup>1</sup>Department of Electrical Engineering, Najafabad Branch, Islamic Azad University  
Najafabad, Isfahan, Iran, shahgholian@iaun.ac.ir

<sup>2</sup>Department of Electrical Engineering, Naein Branch, Islamic Azad University  
Naein, Isfahan, Iran, meh\_mahdavian@yahoo.com

<sup>3</sup>Young Researchers and Elite Club, Central Tehran Branch, Islamic Azad University, Tehran, Iran

**Abstract**—The main operation of power system stabilizer (PSS) is to provide optimal damping which is in phase with the rotor oscillation. In this paper the effect of the transient gain reduction (TGR) on the damping performance and the electromechanical torque components in power system with PSS is proved. The tuning of PSS parameters are computed using phase compensation technique (PCT). Several simulations have been done to show the effect of the TGR on the small signal stability under operating at different loading conditions.

**Keywords**—power system stabilizer; power system stability; small signal model.

## I. INTRODUCTION

Nowadays, with the expansion of the transmission system and increase power transfer through the transmission lines, maintain the dynamic stability of the power system is important [1, 2]. Dynamic instability due to imbalance between the mechanical power input and electrical power output and lack of damping torque is achieved [3, 4]. There are several different ways how to suppressing the low-frequency oscillation of the power system to improve the dynamic stability in a power system [5, 6]. Generally, there are two kinds of power oscillation damping controllers in power systems: PSS and flexible ac transmission systems (FACTS) controllers [7, 8]. PSS is widely used in modern power systems damping the low frequency oscillations in order to the enhancement of the dynamic stability of power systems [9, 10]. Different methods have been used for the design of PSS parameters. A computational technique for the phase shaping of the PSS in a power system to improve the damping of the generator rotor oscillations is presented in [11]. The damping scale is proposed in [12] and formulated to obtain a set of optimal PSS parameters as an objective function to increase system damping after the system undergoes a disturbance. The optimal design of settings of PSS parameters that shift the system eigenvalues associated with the electromechanical modes to the left in the s-plane using evolutionary programming optimization technique is presented in [13]. By using the flexible structure of linear matrix inequalities (LMI), an algorithm that minimizes the norm of the controllers gain matrix while it guarantees the damping factor specified for the closed loop system is presented in [14].

In [15], a hybrid technique for tuning and placement of PSS in power systems is provided to improving power system dynamic stability with wide range of changes in system parameters and operating point of the system. An adaptive fuzzy PSS based on robust synergetic control theory and terminal attractor techniques is developed in [16], which fuzzy logic systems are used to approximate the unknown power system dynamic functions without calling upon usual model linearization and simplifications.

Rotor angle stability is results of a balance between the damping torque (in phase with rotor angle change) and the synchronizing torque (in phase with the speed deviation change). In general, the angle instability may happen due to lack of damping torque (oscillatory instability) or insufficient synchronizing torque (non-oscillatory instability) [17]. In this paper, the effects of TGR using eigenvalues analysis on PSS parameters and rotor angle stability in power system is presented. The phase compensation technique is used to PSS parameters settings. Eigenvalues analysis and time domain simulation show the effectiveness of the TGR under different proposed cases.

## II. POWER SYSTEM MODEL

The block diagram of the linearized small perturbation of the single-machine infinite-bus (SMIB) power system with PSS and TGR is show in Fig. 1, in which case the generator rotor speed deviation is used as the only stabilizing signal. The transfer functions of PSS, TGR and exciter system are  $G_P(s)$ ,  $G_T(s)$  and  $G_V(s)$ , respectively.

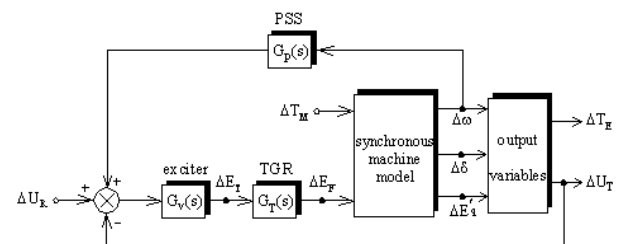


Fig. 1. Control structure for a single-machine infinite-bus power system with TGR and PSS

The state variables are angle load ( $\delta$ ), field voltage ( $E_T$ ), output of TGR ( $E_F$ ), angular velocity ( $\omega$ ) and voltage proportional to direct axis flux linkages ( $E'_q$ ), and the inputs signals are mechanical torque input ( $P_M$ ) and reference voltage ( $U_R$ ) [18].

#### A. Transient Gain Reduction

TGR is used to reduce high frequency gain of the exciter system. The block of the TGR sets after exciter system, so its output signal is  $\Delta E_F$ . By using the lead-lag network, the transfer function of TGR is given by [19]:

$$G_T(s) = \frac{1+T_B s}{1+T_C s} \quad (1)$$

where  $T_B$  and  $T_C$  are transient constant time and steady state constant time, respectively. Usually their values are 1s and 10 s. The phase characteristics of the TGR is show in Fig. 2. The figure shows that the maximum phase lagging of the TGR is approximately -55 degree at 0.3 rad/s.

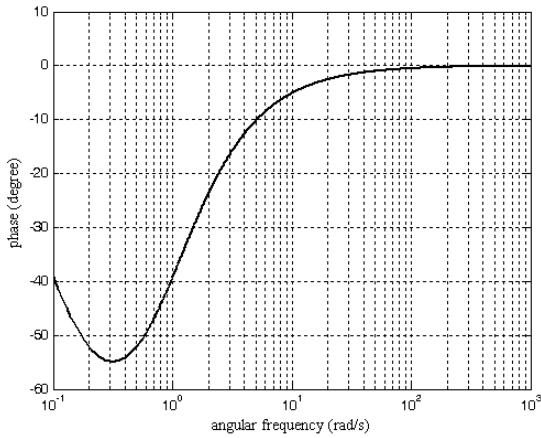


Fig. 2. Phase characteristics of the TGR

#### B. Power System Stabilizer

The transfer function of PSS as shown in Fig. 3 is given by [20, 21]:

$$G_P(s) = K_P \frac{T_W s}{1+T_W s} \left( \frac{1+T_D s}{1+T_G s} \right)^n \quad T_D > T_G \quad (2)$$

where  $K_P$  is the stabilizer gain,  $T_W$  is the washout filter time constant,  $T_D$  is the phase-lead time constants,  $T_G$  is the phase-lag time constants and  $n$  is the number of lead-lag stages [22]. The parameters of lead-lag PSS to be optimized are  $K_P$  and  $T_D$ . The phase characteristics of the PSS for different values of  $T_D$  is show in Fig. 4. The figure shows that the maximum phase lagging of the PSS is between 8 and 55 degree for  $n=1$  and between 10 and 78 degree for  $n=2$ .

#### C. State Space Equation

In this section, IEEE model (1.0) is assumed for synchronous generator by neglecting damper windings with high gain, low time constant static exciter [23]. The 8th order state variables are expressed as:

$$X = [\delta \quad \omega \quad E'_q \quad E_F \quad E_T \quad U_T \quad U_W \quad U_P \quad U_S]^T \quad (3)$$

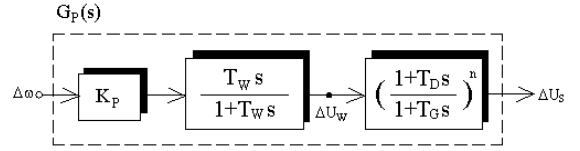
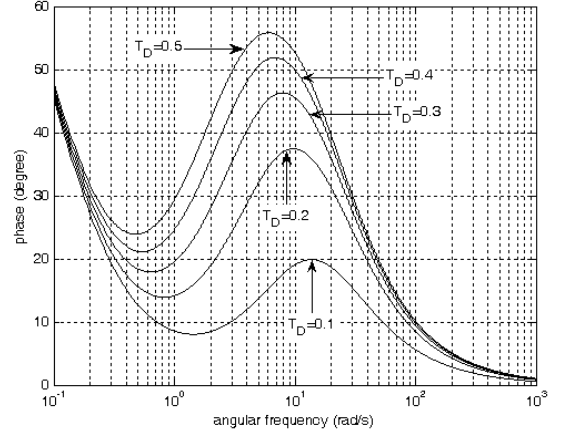
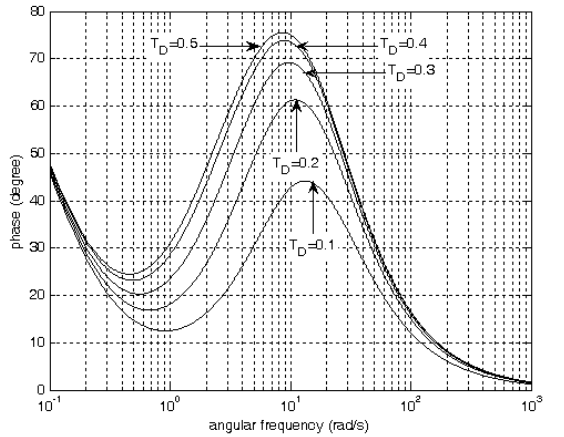


Fig. 3. Block diagram of the conventional PSS

The dynamic equations of the SMIB power system through an external reactance ( $X_E$ ) can be written as [24, 25]:



(a)  $n=1$



(b)  $n=2$

Fig. 4. Phase characteristics of the PSS for different values of the  $n$  ( $T_G=0.05$  and  $T_W=10$ )

$$\frac{d}{dt} \Delta\delta = \omega_b \Delta\omega \quad (4)$$

$$\frac{d}{dt} \Delta\omega = -\frac{K_1}{J_M} \Delta\delta - \frac{K_D}{J_M} \Delta\omega - \frac{K_2}{J_M} \Delta E'_q + \frac{1}{J_M} \Delta P_M \quad (5)$$

$$\frac{d}{dt} \Delta E'_q = -\frac{K_4}{T'_{do}} \Delta\delta - \frac{1}{K_3 T'_{do}} \Delta E'_q + \frac{1}{T'_{do}} \Delta E_F \quad (6)$$

$$\frac{d}{dt} \Delta E_T = \frac{K_A}{T_A} \Delta U_R - \frac{K_5 K_A}{T_A} \Delta\delta - \frac{K_6 K_A}{T_A} \Delta E'_q - \frac{1}{T_A} \Delta E_T \quad (7)$$

$$\frac{d}{dt} \Delta E_F = -\frac{1}{T_C} \Delta E_F + \frac{1}{T_C} \Delta E_T + \frac{T_B}{T_C} \frac{d}{dt} \Delta E_T \quad (8)$$

$$\frac{d}{dt} \Delta U_W = -\frac{1}{T_W} \Delta U_W + K_P \frac{d}{dt} \Delta \omega \quad (9)$$

$$\frac{d}{dt} \Delta U_P = -\frac{1}{T_G} \Delta U_P + \frac{1}{T_G} \Delta U_W + \frac{T_D}{T_G} \frac{d}{dt} \Delta U_W \quad (10)$$

$$\frac{d}{dt} \Delta U_S = -\frac{1}{T_G} \Delta U_S + \frac{1}{T_G} \Delta U_P + \frac{T_D}{T_G} \frac{d}{dt} \Delta U_P \quad (11)$$

$K_1$  and  $K_2$  are the constant derived from electrical torque,  $K_3$  and  $K_4$  are the constant derived from field voltage equation, and  $K_5$  and  $K_6$  are the constant derived from terminal voltage magnitude. By varying the operating at loading conditions, the parameter values  $K_1$ - $K_6$  also vary [26]. Also,  $J_M$  is the generator inertia constant,  $K_D$  is the inherent damping constant,  $T_{do}$  is the d-axis open circuit transient time constant, and  $\omega_b$  is the base electrical angular velocity.  $K_A$  and  $T_A$  are the gain and time constant of the excitation system respectively.

The nominal parameters of the power system and the various loading conditions are given in Table 1. Table 2 summarizes the value of the  $K$  constant under normal load operation and heavy load operation. The steady state operating points of the model power system as a function load conditions is shown in Table 3.

TABLE I. SYSTEM PARAMETERS AND OPERATION DATA

Generator	$J_M=10$ , $X_d=1.6$ , $X'_d=0.32$ , $X_q=1.55$ , $T'_{do}=6$ s, $f=50$ Hz
IEEE type-DC1 excitation system	$K_A=50$ , $T_A=0.05$ s
normal load operation	$P=0.8$ , $Q=0.6$ , $U_t=1$
heavy load operation	$P=1.5$ , $Q=1.1$ , $U_t=1$
transient gain reduction	$T_B=1$ , $T_C=10$
lead-lag PSS	$T_W=10$ s, $T_2=T_4=0.05$ s
transmission line reactance	$X_E=0.4$
un-damped natural frequency	$\omega_n=5.4741$ rad/s

TABLE II. PARAMETERS K VALUES (PU)

Constants	Normal load operation	Heavy load operation
$K_1$	0.9538	0.6506
$K_2$	0.9445	1.1389
$K_3$	0.3600	0.3600
$K_4$	1.2089	1.4579
$K_5$	-0.0539	-0.2590
$K_6$	0.4674	0.4213

TABLE III. STEADY STATE OPERATION POINT (PU)

Item	Normal load operation	Heavy load operation
$U_{do}$	0.5405	0.6518
$U_{qo}$	0.8413	0.7584
$I_{do}$	0.9400	1.8119
$I_{qo}$	0.3500	0.4205
$E'_{qo}$	1.1400	1.3382
$\delta_o$	55.55°	87.6568

### III. DESIGN OF PSS USING PHASE COMPENSATION TECHNIQUE

The change in the electrical torque deviation can be expressed in terms of rotor angle and voltage reference deviations:

$$\Delta T_E(s) = K_1 \Delta \delta + K_2 \Delta E'_q(s) = K_1 \Delta \delta + H_Q(s) \Delta \delta + H_P(s) \Delta \delta + G_E(s) \Delta U_R(s) \quad (12)$$

where  $H_Q(s)$  is the control transfer function (between the output electrical torque and load angle),  $G_E(s)$  is the electrical loop transfer function (between exciter input and the output electrical torque) and  $H_P(s)$  is the PSS transfer function (between the output electrical torque  $\Delta T_{E2}$  and input signal of PSS). The block diagram representing the small signal stability model can be simplified as shown in Fig. 5. The expression for the transfer function of electrical loop as shown in Fig. 6 is given by (without PSS):

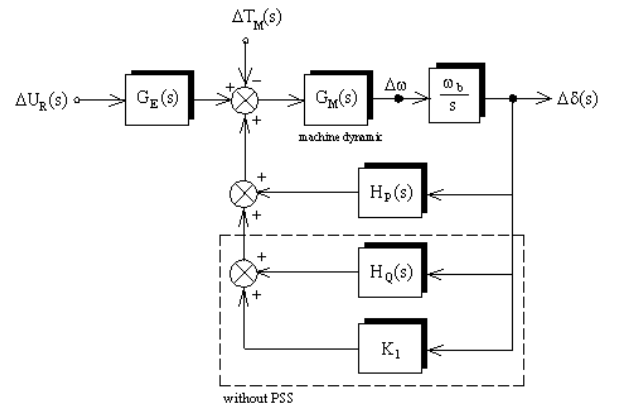


Fig. 5. Block diagram of SMIB power system

$$G_E(s) = K_2 \frac{\Delta E'_q}{\Delta U_R} = \frac{K_2 G_F(s) G_V(s) G_T(s)}{1 + K_6 G_F(s) G_V(s) G_T(s)} \quad (13)$$

The electrical transfer function is dependent to parameters  $K_2$ ,  $K_3$  and  $K_6$ . Parameter  $K_3$  is independent of the load change, but  $K_2$  and  $K_6$  have slowly change for changes in the load. Therefore there is no effect on response frequency transfer function  $G_E(s)$ . The effect of the TGR on phase lagging characteristics of the  $G_E(s)$  is show in Fig. 7 under normal load operation. The figure shows that the maximum phase lagging of the system without TGR and with TGR are approximately -28 and -93 degree at 2 rad/s, respectively. The transfer function due the PSS is given by:

$$H_P(s) = \frac{s}{\omega_b} G_E(s) G_P(s) \quad (14)$$

The phase of the electrical loop transfer function is negative but the phase of the PSS is positive. In the phase compensation technique, the amplitude of synchronizing torque component due of the PSS is minimum. Also the phase of the transfer function of the PSS is compensated with the phase of the electrical loop transfer function [27]. Therefore the real of the  $H_P(j\omega)$  in the electromechanical mode natural frequency of

oscillation ( $\omega_n$ ) is zero. The damping torque component is occurred by PSS is:

$$K_{d(PSS)}(\omega) = \frac{\omega_b}{\omega} \text{Im}[H_p(j\omega)] \quad (15)$$

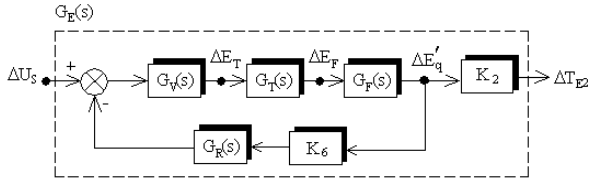


Fig. 6. Block diagram of the electrical loop

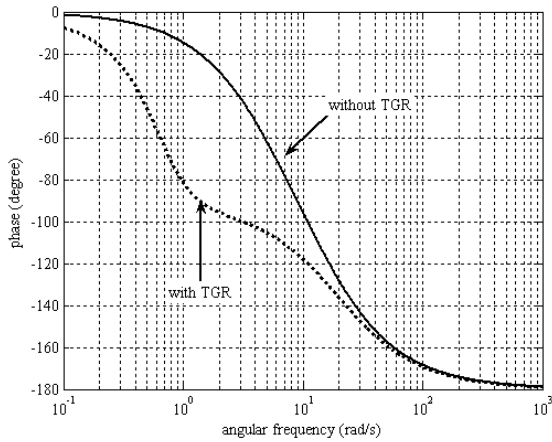


Fig. 7. Effect of TGR on phase lagging characteristics of the electrical transfer function under normal load operation

#### IV. SIMULATION RESULTS

In this section two types of system have been considered for analysis: the power system without TGR and the power system equipped with TGR. The method for the PSS design parameters is based on the phase compensation technique. The results are compared with integral of squared error (ISE) technique in [19]. The system eigenvalues without the TGR for nominal and heavy loading conditions are given in Table 4 and Table 5 respectively. The real part and the imaginary part of the eigenvalue represent the damping mode and the damped natural frequency of oscillation respectively. It is observed that the electromechanical mode for the open-loop system without TGR which are characterized by the eigenvalues  $0.1028 \pm j5.5022$  and  $0.8556 \pm j5.1274$  are poorly damped. The system eigenvalues with the TGR for nominal and heavy loading conditions are given in Table 6 and Table 7 respectively. A comparison of the rotor angle deviation and angular speed deviation of the SMIB power system without TGR and equipped with PSS is shown in Fig. 8. The system eigenvalues with the TGR for nominal loading and heavy loading condition are given in Table 8 and Table 9 respectively. A comparison of the rotor angle deviation and electrical torque deviation of the SMIB power system with TGR and equipped with PSS for normal load is shown in Fig. 9.

TABLE IV. SYSTEM EIGENVALUES WITHOUT TGR FOR NORMAL LOAD OPERATION

Without PSS	With PSS Phase compensation technique ( $K_P=26.97, T_I=0.19$ )	With PSS ISE technique [19] ( $K_P=38.65, T_I=0.11$ )
$0.1028 \pm j5.5022$	$-3.4217 \pm j4.5810$	$-9.9010 \pm j3.9282$
-14.2975	$-7.0777 \pm j9.4812$	$-3.1956 \pm j8.4712$
-6.3710	-32.0598	-30.4614
---	-7.4029	-3.8061
---	-0.1016	-0.1023

TABLE V. SYSTEM EIGENVALUES WITHOUT TGR FOR HEAVY LOAD OPERATION

Without PSS	With PSS Phase compensation technique ( $K_P=26.97, T_I=0.19$ )	With PSS ISE technique [19] ( $K_P=38.65, T_I=0.11$ )
$0.8556 \pm j5.1274$	$-1.5553 \pm j3.8217$	$-8.3076 \pm j4.0067$
-7.6106	$-6.8162 \pm j15.2560$	$-3.3305 \pm j8.0389$
-14.5635	-37.0282	-31.4121
---	-6.6902	-5.7727
---	-0.1017	-0.1026

TABLE VI. SYSTEM EIGENVALUES WITH TGR FOR NORMAL LOAD OPERATION

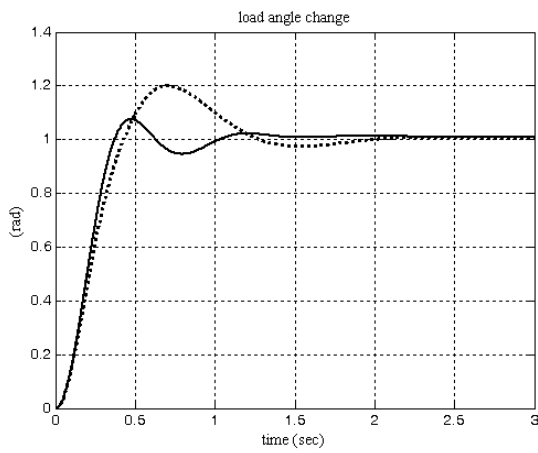
Without PSS	With PSS Phase compensation technique ( $K_P=35.25, T_I=0.45$ )	With PSS ISE technique [19] ( $K_P=35.50, T_I=0.12$ )
$-0.0801 \pm j5.4542$	$-1.5660 \pm j4.9212$	$-0.1960 \pm j5.7712$
$-0.3969 \pm j0.5615$	$-0.3815 \pm j0.5249$	$-0.3975 \pm j0.5128$
-19.6090	$-10.5522 \pm j12.6256$	$-17.1740 \pm j3.5163$
---	-0.1020	-0.1022
---	-35.5615	-25.0258

TABLE VII. SYSTEM EIGENVALUES WITH TGR FOR HEAVY LOAD OPERATION

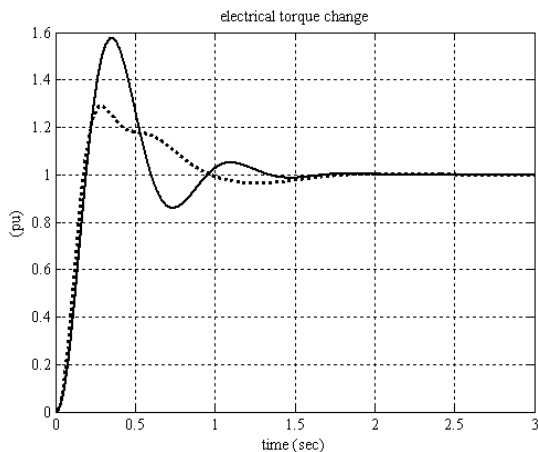
Without PSS	With PSS Phase compensation technique ( $K_P=35.25, T_I=0.45$ )	With PSS ISE technique [19] ( $K_P=35.50, T_I=0.12$ )
$-0.0275 \pm j4.4345$	$-1.4951 \pm j3.8684$	$-0.1801 \pm j4.8762$
$-0.4380 \pm j0.7642$	$-0.3943 \pm j0.6996$	$-0.4309 \pm j0.6749$
-19.6320	$-10.0681 \pm j13.6788$	$-16.9586 \pm j3.7488$
---	-0.1022	-0.1023
---	-35.5615	-25.4214

#### V. CONCLUSIONS

Power system stability is one of the most important problems in power system operation and control. PSS is used to improve the dynamic stability of power systems. In this paper, the method for the PSS design parameters is based on the phase compensation technique. The linearized model of single-machine infinite-bus power system which includes the effect of TGR and PSS has been adopted. The effects of TGR using eigenvalues analysis and simulation on power systems small signal stability is shown.

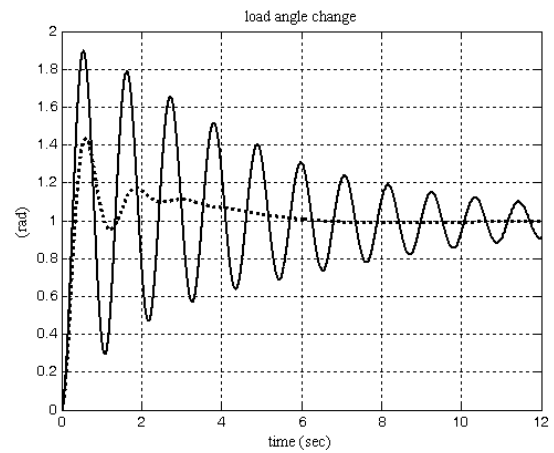


(a) Rotor angle deviation

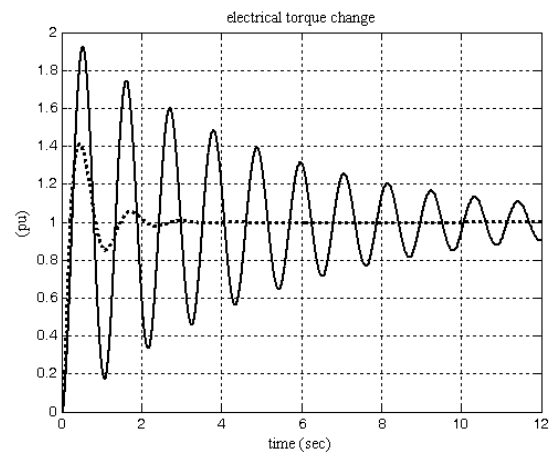


(b) Electrical torque deviation

Fig. 8. The response of system equipped with PSS under normal load operation: PCT method (dot), ISE method (solid)



(a) Rotor angle deviation



(b) Electrical torque deviation

Fig. 9. The response of system equipped with TGR and PSS under normal load operation: PCT method (dot), ISE method (solid)

## REFERENCES

- [1] Gh. Shahgholian, A. Movahedi, "Power system stabiliser and flexible alternating current transmission systems controller coordinated design using adaptive velocity update relaxation particle swarm optimisation algorithm in multi-machine power system", *IET Gener. Transm. Distrib.*, Vol. 10, No. 8, pp. 1860-1868, May. 2016.
- [2] J. Faiz, Gh. Shahgholian, M. Torabiyani, "Design and simulation of UPFC for enhancement of power quality in transmission lines", *Proceeding of the IEEE/POWERCON*, pp. 1-5, Hangzhou, Oct. 2010.
- [3] Gh. Shahgholian, A. Movahedi, "Coordinated design of thyristor controlled series capacitor and power system stabilizer controllers using velocity update relaxation particle swarm optimization for two-machine power system stability", *Revue Roumaine Des Sciences Techniques*, Vol. 59, No. 3, pp. 291-301, 2014.
- [4] Gh. Shahgholian, "Development of state space model and control of the STATCOM for improvement of damping in a single-machine infinite-bus", *International Review of Electrical Engineering*, Vol.4, No.6, pp.1367-1375, Nov./Dec. 2009.
- [5] Gh. Shahgholian, E. Haghjoo, A. Seifi, I. Hassanzadeh, "The improvement DSTATCOM to enhance the quality of power using fuzzy-neural controller", *Journal of Intelligent Procedures in Electrical Technology*, Vol. 2, No. 6, pp. 3-16, Summer 2011 (in Persian).
- [6] S. Shojaeian, J. Soltani, "Low frequency oscillations damping of power system including unified power flow controller based on adaptive backstepping control", *Rev. Roum. Sci. Techn.*, Vol. 58, No. 2, pp. 193-204, 2013.
- [7] Y.J. Lin, "Proportional plus derivative output feedback based fuzzy logic power system stabilizer", *Elec. Power and Ene. Sys.*, Vol. 44, pp. 301-307, 2013.
- [8] Gh. shahgholian, A. Etesami, "The effect of thyristor controlled series compensator on power system oscillation damping control", *Int. Rev. of Ele. Eng.*, Vol.5, No.2, pp. 1822-1830, Aug. 2011.
- [9] H. Barati, R. Saki, S.S. Mortazavi, "Intelligent control of UPFC for enhancing transient stability on multi-machine power systems", *Jou. of Inte. Proc. in Elect. Tech.*, Vol. 1, No. 1, pp. 3-12, Winter 2010.
- [10] Gh. Shahgholian, J. Faiz, "The effect of power system stabilizer on small signal stability in single-machine infinite-bus", *Int. Journal of Elect. and Eng.*, Vol. 4, No. 2, pp.45-53, 2010.
- [11] F. DeMarco, N. Martins, J.C.R. Ferraz, "An automatic method for power system stabilizers phase compensation design", *IEEE Trans. on Pow. Sys.*, Vol. 28, No. 2, pp. 997-1007, May 2013.
- [12] S.K. Wang, "A novel objective function and algorithm for optimal PSS parameter design in a multi-machine power system", *IEEE Trans. on Pow. Sys.*, pp. 522-531, Feb. 2013.
- [13] M.A. Abido, "Optimal design of power system stabilizers using particle swarm optimization", *IEEE Trans. on Ene. Con.*, pp.429-436, Vol.17, No.4, Dec. 2002.
- [14] V.A.F. de Campos, J.J. da Cruz, L.C. Zanetta Jr., "Robust and optimal adjustment of power system stabilizers through Linear matrix inequalities", *Elec. Pow. and Ene. Sys.*, Vol. 42, pp. 478-486, 2012.
- [15] V. Keumarsi, M. Simab, Gh. Shahgholian, "An integrated approach for optimal placement and tuning of power system stabilizer in multi-machine systems", *International Journal of Electrical Power and Energy Systems*, Vol. 63, pp. 132-139, Dec. 2014.

- [16] Z. Bouchama, N. Essounbouli, M.N. Harmas, A. Hamzaoui, K. Saoudi, "Reaching phase free adaptive fuzzy synergetic power system stabilizer", *International Journal of Electrical Power and Energy Systems*, Vol. 77, pp. 43–49, May 2016.
- [17] H. Ghasemi, "On-line monitoring and oscillatory stability margin prediction in power systems based on system identification", PhD Thesis, Waterloo, Ontario, Canada, 2006.
- [18] Gh. Shahgholian, P. Shafaghi, S. Moalem, M. Mahdavian, "Analysis and design of a linear quadratic regulator control for static synchronous compensator", *Proceeding of the IEEE/ICCEE*, pp.65-69, Dubai, Dec. 2009.
- [19] K. Bhattacharya, J. Nanda, M.L. Kothari, "Optimization and performance analysis of conventional power system stabilizers", *Elec. Pow. & Ene. Syst.*, Vol.19, No.7, pp.449-458, 1997.
- [20] Z. Jiang, "Design of a nonlinear power system stabilizer using synergetic control theory", *Elec. Pow. Sys. Res.*, Vol. 79, No. 6, pp. 855-862, June 2009.
- [21] Gh. Shahgholian, "Review of power system stabilizer: Application, modeling, analysis and control strategy", *Int. J. on Technical and Physical Problems of Eng.*, Vol. 5, No. 3, pp. 41-52, Sep. 2013.
- [22] D.D. Simfukwe, B.C. Pal, R.A. Jabr, N. Martins, "Robust and low-order design of flexible ac transmission systems and power system stabilizers for oscillation damping", *IET Gen., Trans. and Dist.*, Vol.6, No.5, pp.445-452, 2012.
- [23] G. Guraala, I. Sen, "Power system stabilizers design for interconnected power systems", *IEEE Trans. on Pow. Sys.*, Vol.25, No.2, pp.1042-1051, May 2010.
- [24] M.A. Mahmud, M.J. Hossain, H.R. Pota, "Transient stability enhancement of multimachine power system using nonlinear observer-based excitation controller", *Ele. Pow. and Ene. Sys.*, Vol. 58, pp. 57-63, 2014.
- [25] M.A. Mahmud, H.R. Pota, M. Aldeen, M.J. Hossain, "Partial feedback linearizing excitation controller for multimachine power systems to improve transient stability", *IEEE Trans. on Pow. Sys.*, Vol. 29, No. 2, pp. 561-571, March 2014.
- [26] A. Andreoiu, "On power system stabilizer: Genetic algorithm based tuning and economic worth as ancillary services", PhD. Thesis, Goteborg, Sweden, 2004.
- [27] M. Sekita, Y.Xia, M.Shimomura, "A new design for digital PSS", *IEEE/ICPST*, pp.795-799, Aug. 1998.